Egyptian Journal of Chemistry

http://ejchem.journals.ekb.eg/

Preparation and Characterization of Borosilicate Bioglass

Walla M. Awad[1,*], Amr M. Abdelghany[2, 3] and Mahrous S. Meikhail[1]

[1]*Physics Department, Faculty of Science, Mansoura University, 35516, Mansoura, Egypt*

[2]*Spectroscopy department, Physics Division, National Research Center, 33 ElBehouth St., 12311 Dokki, Giza, Egypt*

[3] *Basic Science Department, Horus University, International Coastal Rd, New Damietta, KafrSaad, Damietta, Egypt*

Abstract

Bioglass with the composition of SiO_2-B_2O_3-24.5CaO-24.5Na_2O–6P_2O_5 by varying B_2O_3 content on SiO_2 content using the conventional melt-quenching technique. Bioglass was analyzed using X-ray diffraction, Ultraviolet (UV-Vis) spectroscopy, and Fourier transforms infrared (FTIR). Tested samples were subjected to a two-step-controlled crystallization route to obtain their respective glass-ceramic derivatives. The crystalline nature of the glass-ceramic was tested via x-ray diffraction analysis. FTIR spectral data of analyzed samples before and after controlled crystallization. Optical absorption spectral data was used to estimate different physical parameters associated with the compositional variation of boron atoms at the expense of silicon atoms. Density, molar volume, molecular mobility, average boron–boron, boron atom molar volume, ion concentration, polaron radius, and field strength were also estimated and correlated to the structural variations.

Keywords: Borosilicate; Bio-glass; heat treatment; FTIR; XRD

1. Introduction

New materials that stimulate a biochemical reaction in live tissue to create a strong chemical connection with biological fixation between the tissue and the prosthesis have recently been developed [1, 2]. The oldest bioactive material is bioactive modified soda-lime-silica glass 45S5, which was first published by Hench et al. in 1971 [3] and is today a well-characterized material with applications in a variety of biomedical fields [4–6].

Bioactive glasses are chemically connected to bone and may be easily replaced by bone; these properties make them a potentially useful medicinal material. New bioactive glass applications need not only strict bioactivity monitoring but also a thorough understanding of the impact of glass composition on its synthesis and structure in a variety of products. Bioactive glasses can link with both hard and soft tissue in vivo or in vitro by forming a surface layer of hydroxycarbonate apatite by transferring ionic species from the bulk material [7]. Glass reactivity in aqueous solutions is significantly influenced by the glass structure, which is one of the elements to consider when choosing a synthesis. Bioactive glasses (BGs) and bioactive glass-ceramics (BGCs) are being studied for a variety of medicinal uses, including bone tissue development and repair [8]. When BGs and BGCs were placed in a simulated biological environment, they formed a bone-like hydroxyapatite (HA) covering on their surface [9]. This has also been demonstrated in vivo [10]. Bone formation, such as HA, is a crucial component for establishing a robust interfacial contact between implants and bone [11]. It is widely assumed that the HCA layer is produced on the surface of the bioactive glass implant as a result of a reaction sequence defined by Hench [12], including ion exchange processes combined with a change in pH and the formation of a silica-rich layer. These steps are followed by dissolution and migration of Ca^{2+} and $(PO_4)^{-3}$ ions from the glass through the SiO^{-2} rich layer and from the solution, resulting in the formation of the SiO^{-2} rich layer of amorphous calcium phosphate (ACP) layer.

The adsorption of growth factors with the early development of the HCA layer, supported by osteoprogenitor cell attachment, proliferation, and differentiation, is considered to be one of the basic processes of bone-bonding [13]. Osteoblasts (bone-forming cells) create an extracellular matrix (collagen) that mineralizes and converts as the glass

*Corresponding author e-mail: w.mhmd@yahoo.com.(Walla M. Awad)

Receive Date: 04 November 2021, Revise Date: 27 November 2021, Accept Date: 07 December 2021, First Publish Date: 07 December 2021

DOI: 10.21608/EJCHEM.2021.104384.4818

degrades and converts over time, resulting in a nanocrystalline mineral and collagen on the glass implant's surface [14]. It has long been known that 45S5 glass is biocompatible [15].

On the other hand, the modest rate of degradation of silicate-based BG makes it difficult to synchronize the rate of BG scaffold degradation to the rate of new tissue formation [16, 17]. In vitro cell, proliferation and differentiation, as well as tissue penetration in vivo, be aided by borate bioactive glasses [18]. Borate bioactive glasses are effective in the treatment of bone infections as a drug release substrate. A concern connected with the bioactive glass of borate is the toxicity of boron released as borate ions $(BO_3)^{-3}$ into the solution. Some borate glasses are hazardous to cells under typical static in vitro culture settings, although toxicity has decreased under dynamic culture circumstances. Recent research has demonstrated the capacity to control the pace of deterioration of bioactive glass by manipulating its structure. For example, partial replacement of SiO_2 in silicate 45S5 or 13-93 glass with B_2O_3 (borosilicate bioactive glass) or total replacement of SiO_2 with B_2O_3 might result in a wide variety of degradation rates (borate bioactive glass). Controlling the glass composition can help to balance the pace of degradation of borate-based bioactive glass with the rate of bone repair.

The presented work aims to introduce a borate glass former partner to control dissolution rate, reduce the time of hydroxyapatite formation, and increase the glass bonding ability, in addition to optimizing the bone-bonding criteria of the studied glassy system.

2. Experimental work

2.1. Sample preparation

Glass samples were formed using analytical grade chemicals of silicon dioxide SiO_2 supplied by LANXESS, Germany. Boron oxide is used in the form of boric acid H_3BO_3 supplied by El-Gomhouria Co. P_2O_5 was introduced in the form of Ammonium dihydrogen orthophosphate supplied by LANXESS Co. CaO and Na_2O were introduced in their carbonate form and supplied by EL-Nasr pharmaceutical chemicals Co. All the previously mentioned chemicals were used to synthesize glassy samples with a nominal composition of$x$$SiO_2$- (45-$x$) B_2O_3-24.5 Na_2O-24.5 CaO-6 P_2O_5, as listed in **Table (1)**. The batches were melted in porcelain crucibles within a programmable electrical furnace regulated at 1100–1200 ºC. Molten glass was occasionally stirred many times to ensure the formation of homogenized bubble-free glasses. To eliminate thermal and internal stresses, the molten glass was cast onto warmed stainless-steel plates of the appropriate size, annealed for 1 hour, and then cooled gently to room temperature.

Table (1) Notation and structure of samples

Sample	Composition				
	SiO_2	B_2O_3	CaO	Na_2O	P_2O_5
B0	45	0	24.5	24.5	6
B5	40	5	24.5	24.5	6
B10	35	10	24.5	24.5	6
B15	30	15	24.5	24.5	6
B20	25	20	24.5	24.5	6
B25	20	25	24.5	24.5	6
B30	15	30	24.5	24.5	6
B35	10	35	24.5	24.5	6
B40	5	40	24.5	24.5	6
B45	0	45	24.5	24.5	6

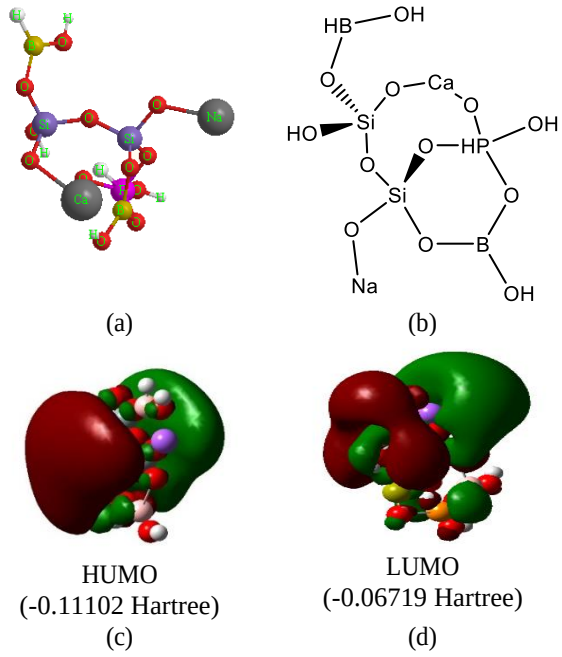

Figure (1) Graphical representation of the mechanism of interaction (a, b, c, d refer to 3D, 2D, HOMO, LUMO of borosilicate bioactive glass respectively)

2.2.Physical measurements

X-ray diffraction patterns, Fourier transforms infrared (FTIR), ultraviolet (UV-vis) spectroscopy and crystallization events have all been used to study bioglass samples. For the preparation of glass ceramics, heat treatment was employed to regulate crystallization. After higher heat treatment temperatures (800-900°C), X-ray diffraction analysis and Fourier transform infrared spectroscopy were demonstrated.

Xylene was used as an immersion solvent to determine the density of the examined glasses. The glass density (ρ) was measured at room temperature (30 °C) using Archimedes' method. Using a digital balance, a bulk solid sample was weighed in air (WSA) and the solvent (WSL), and density was estimated as the average of triplicate readings using

the formula [19]:

$$\rho = \frac{W_{SA}}{W_{SA}-W_{SL}}\rho_L \quad (1)$$

where ρ_L denotes sample density.
The predicted V_m of the synthesized glass samples:

$$V_m = \sum_i \frac{n_i M_i}{\rho} \quad (2)$$

where M_i denotes the molecular mass of a component n_i denotes the molar ratio, and ρ is the sample density.

The V_f is used to describe molecular mobility within a network and is defined as the vacant space between molecules calculated using the formula:

$$V_f = V_m - \sum_i V_i X_i \quad (3)$$

The molar ratio of the samples is Xi, and the V_m of each component is Vi. The ratio of the ions' lowest fraction of volume occupied to the corresponding effective volume of glass computed using [20] was defined as Pd [20]:

$$Pd = \sum_i \frac{V_i X_i}{V_m} \quad (4)$$

The impact of dopant concentration in the glass matrix may also be evaluated using average boron–boron separation [21]:

$$\text{db-b}=\left[\frac{V_m^b}{NA}\right]^{\frac{1}{3}} \quad (5)$$

whereV_m^b is the boron atoms' molar volume and is provided by

$$Vm^b = \left(\frac{Vm}{2\,(1-Xb)}\right) \quad (6)$$

where X_b is the mole percentage of B_2O_3 in the sample.
The ions concentration (N) is calculated using the formula [22]

$$N=\frac{\text{Mol\%of dopant}*\text{Density of sample}*\text{Avogadreo'sNo}}{\text{Glass average molecular mass}} \quad (7)$$

A polaron is a quasi-particle that is used to characterize and grasp the interaction between ions and electrons in materials. Based on the value obtained for N, the polaron radius (rp) in (A °) may be calculated using the formula [23]:

$$\text{rp(Å)}=\left(\frac{1}{N}\right)^{\frac{1}{3}} \quad (8)$$

Equations [24] can be used to calculate the field strength (F):

$$F=\frac{Z}{r_p^2} \quad (9)$$

Where Z is the molar mass (B_2O_3).

3. Results and discussions:

3.1 FTIR Absorption Spectra of borosilicate Bioglass Before and after heat treatment

Figures (2 and 3) show FTIR readings for the produced glass samples before and after heat treatment in the 400–4000 cm^{-1} range. The typical Si–O–Si bond-associated bands appeared at 1031 cm^{-1}. In water molecules, broadband at 3434 cm^{-1} is due to the O-H stretching vibrational modes. Wavenumber 470-480 cm^{-1} refers to the Si-O-Si Bridge's rocking vibration [25, 26]. The B-O-B bond bending of the borate network [27] was correlated with 700-720 cm^{-1}. While the peak observed at 930-1197 cm^{-1} is due to the tensile vibration of the trigonal BO^{-3} units of the tetrahedral (BO^{-4}) units and the band at 1200-1500 cm^{-1} BO stretching vibrations, respectively. The presence of a [BO_3^{-3}] band suggests that [BO_3^{-3}] replaces [SiO_4^{-4}] positions in the glass structure in part.
The areas of the BO_3 and BO_4 peaks were combined to determine the N4 using the following formula:

$$N_4 = \frac{BO_4}{BO_4 + BO_3}$$

Figures (4 and 5) displays FTIR deconvoluted spectral data with residuals of two different samples that were used to calculate the fraction of four coordinated boron. Estimates the BO_4 influence on the change of the relative population of tetrahedral units BO_4 and triangular units BO_3 by plotting N4 as a function of BO_4 content. The levels of N4 were found to vary depending on the concentration of BO_4. It appears that adding BO_3 reduces BO_4 units before heat treatment, while the converse is true after heat treatment.

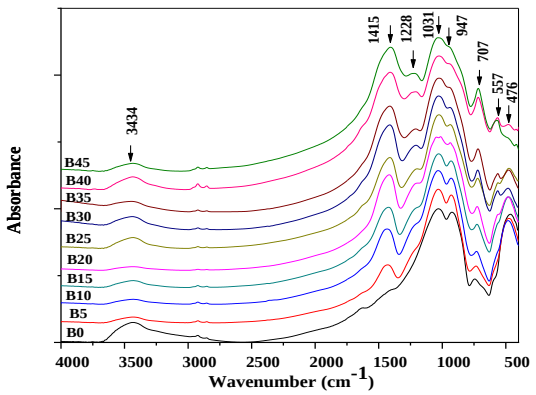

Figure (2) FTIR of borosilicate bioactive glass before heat treatment

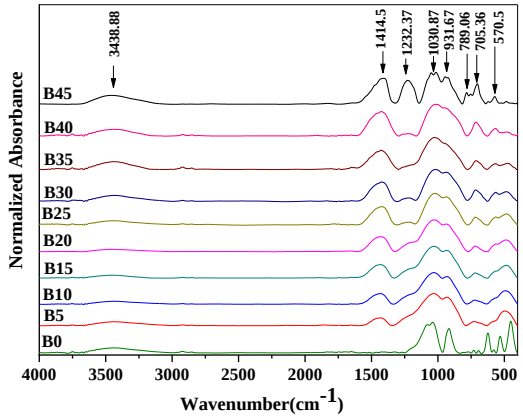

Figure (3) FTIR of borosilicate bioactive glass after heat treatment

3.2 X-ray Diffraction Studies of borosilicate Bioglass

X-ray experimental results for borosilicate bioactive glass before and after heat treatment are shown in Figures (6 and 7). Untreated borosilicate glass behaved as if it were in an amorphous state, which represents the material's inherent instability and glassy nature. Some crystalline phases appear after heat treatment.

3.3 UV-Visible Absorption Spectra of borosilicate bioglass

The optical absorption spectra of the glass samples are presented in Figure (8). In the absorption spectra, the power-law region is visible. In the UV area, there is a high absorption edge. The basic absorption edges aren't as sharp as they could be, as shown in Figure (8). This is a characteristic of most glass materials. A redshift appears as the concentration of PbO and B_2O_3 rises steadily.

Figures (9) the optical bandgap from the absorption at the edge of the optical band gap Eg can be estimated by fitting the following equation:

$$\alpha h\nu = A\left(h\nu - E_g\right)^m$$

Where, m is a constant that depends on the direct or indirect optical band gap, and A is the independent energy constant. For m = 1/2, the bandgap ranged from 3.24 eV to 3.40 eVwhich is shown in Figure(10), Table (2),and represents the directly allowed transition.

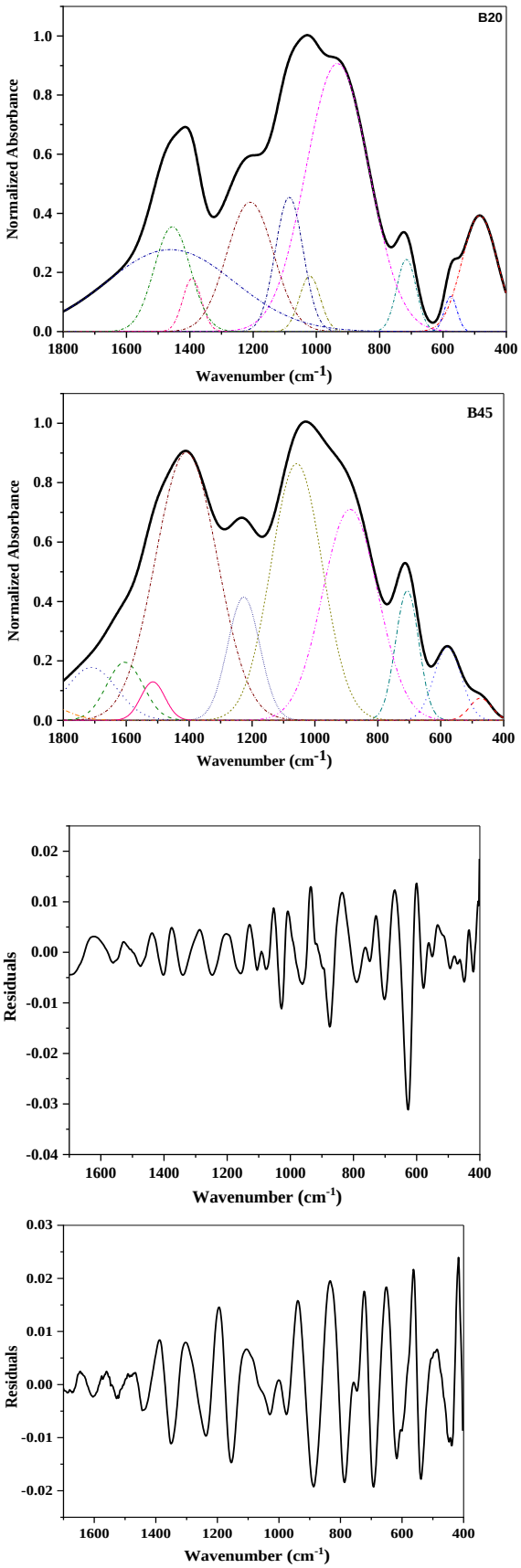

Figure (4) Deconvolution of borosilicate bioactive glass before heat treatment

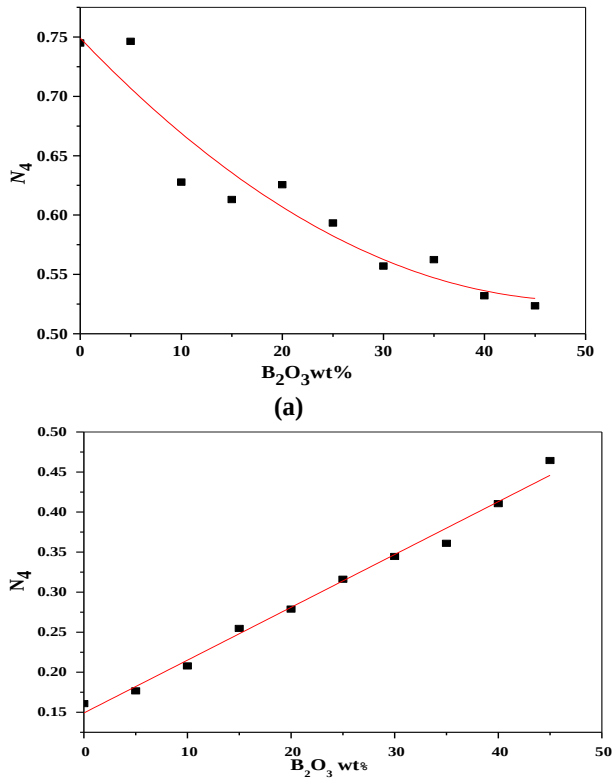

Figure (5) N4 of borosilicate bioactive glass (a) before, and (b) after heat treatment

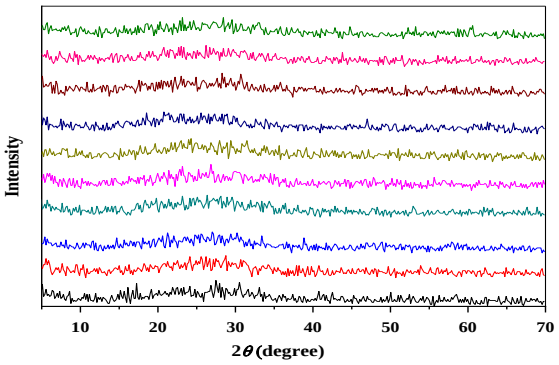

Figure (6) X-ray of borosilicate bioactive glass before heat treatment

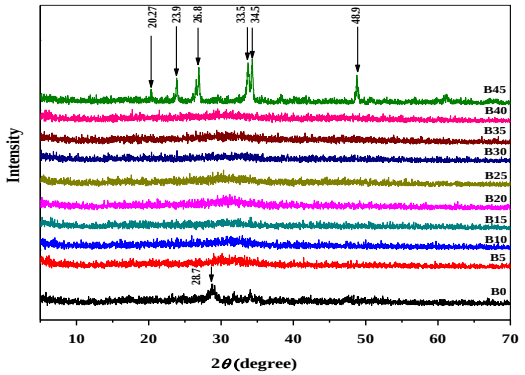

Figure (7) X-ray of borosilicate bioactive glass after heat treatment

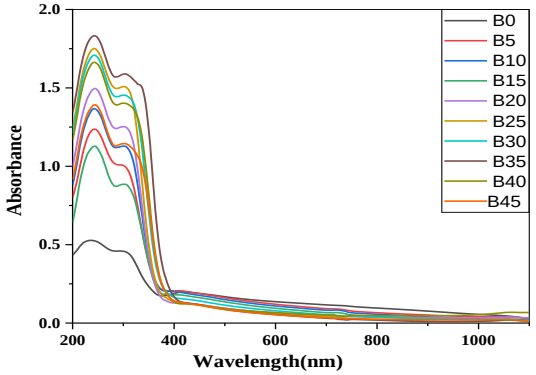

Figure (8) UV-vis experimental data for borosilicate bioactive glass

Table 2 Direct, indirect, and Energy gaps of borosilicate bioactive glass before heat treatment

Sample	Boron Content	λ_{edge}	$E_{Optical}$	E_{Direct}	$E_{Indirect}$
		(nm)	(eV)		
B0	**0.0**	382	3.24	2.63	3.63
B5	**5**	370	3.35	3.01	3.86
B10	**10**	367	3.38	3.05	3.88
B15	**15**	373	3.32	2.98	4.01
B20	**20**	364	3.40	3.11	3.89
B25	**25**	364	3.40	3.15	3.68
B30	**30**	372	3.33	3.08	3.74
B35	**35**	382	3.24	3.06	3.68
B40	**40**	377	3.28	3.06	3.8
B45	**45**	379	3.27	3.01	3.89

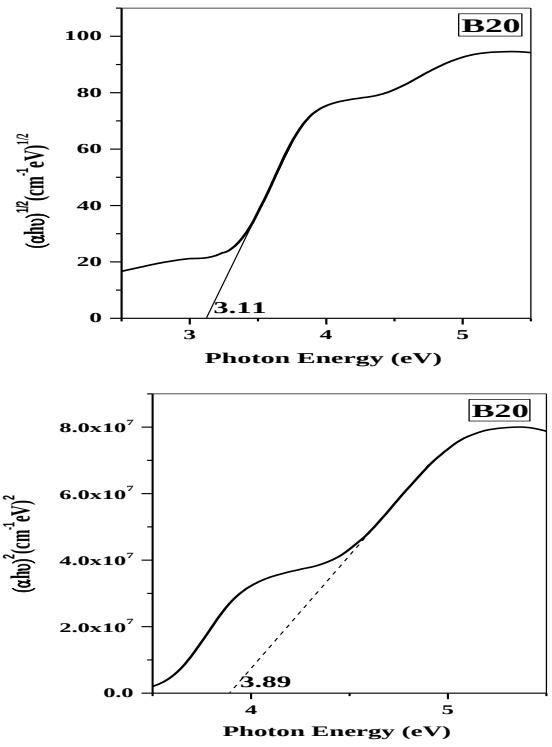

Figure (9) Direct and indirect bandgaps estimation curves of borosilicate bioactive glass

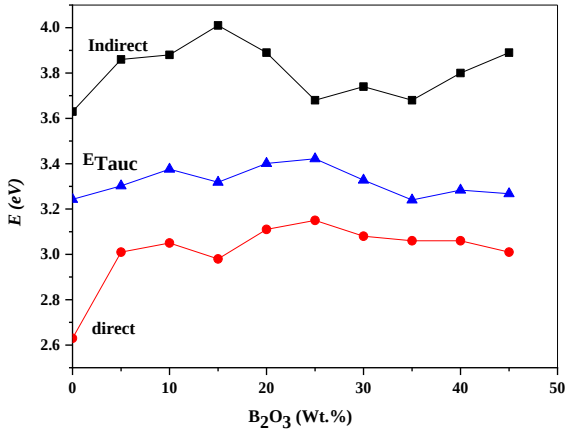

Figure (10) Direct and indirect bandgaps estimation curves of borosilicate bioactive

glasses reveal an amorphous nature while their glass-ceramic derivatives show a high tendency for crystallization approved through XRD analysis. The FTIR spectral data of both glass and glass-ceramics approve the bone-bonding ability of the studied samples with the appearance of separated bands and combined with the variation of the four coordinated boron calculated via the deconvolution analysis technique (DAT).Optical absorption spectral data were recorded and used to estimate the optical energy gap and other physical parameters that are used to interpret and understand several structural variations associated with the increase of boron atoms atthe expense of silicon atoms. The density, Pd, and ri of the prepared samples were found to be decreased with B_2O_3 content, while V_m , V_f, and ion concentration were found to be increased, demonstrating an opposite trend.

Conclusion

Mixed former borosilicate glasses and their glass ceramic derivatives were successfully synthesized via traditional melt quenching and step nucleation and crystallization routes, respectively. Synthesized

Table 3 Physical properties of $45SiO_2$– (45-x) B_2O_3-24.5CaO–24.5Na_2O–6P_2O_5 glasses system

Parameters	Glasscode									
	B0	B5	B10	B15	B20	B25	B30	B35	B40	B45
Density(d_s)gcm^{-3}±0.0002	2.67	2.65	2.62	2.63	2.51	2.49	2.48	2.46	2.46	2.41
Molarvolume(V_m)cm^{3}mol^{-1}±0.0001	24.19	24.53	24.90	25.04	26.40	28.32	29.45	28.41	27.62	28.63
Packingdensity(P_d)	0.53	0.54	0.54	0.55	0.53	0.51	0.50	0.53	0.56	0.55
Freevolume(V_f)	11.32	11.37	11.44	11.27	12.32	13.93	14.74	13.38	12.27	12.94
Averagemol.wt.(M_{Av})(g)	58.23	65.01	65.43	65.91	66.47	70.65	73.02	69.83	67.92	76.33
Ion concentration (N) (10^{+21} ions)	0.00	1.09	2.17	3.26	4.15	4.87	5.67	6.90	8.17	8.94
Polaron radius (rp) (A˚)	0.00	3.91	3.11	2.72	2.51	2.38	2.26	2.12	2.00	1.94
Inter-nuclear distance (ri) (A˚)	0.00	9.71	7.73	6.74	6.22	5.89	5.61	5.26	4.96	4.82
Field strength (F) 10^{+17}(g mol^{-1}cm^{-2})	0.00	2.28	3.59	4.72	5.55	6.17	6.82	7.79	8.71	9.25
MolarvolumeoftheboronatomsV^b	12.09	12.84	13.68	14.48	16.14	18.37	20.37	21.07	22.09	24.89
Averageboron–borondistance(d_{B-B})(nm)	1.26	1.27	1.272	1.274	1.29	1.33	1.35	1.33	1.32	1.33

References

1. Liang W, Rahaman MN, Day DE, Marion NW, Riley GC, Mao JJ (2008) Bioactive borate glass scaffold for bone tissue engineering. J. Non-Cryst. Solids 354:1690-1696.
2. Mariappan CR, Yunos DM, Boccaccini AR, Roling B (2009) Bioactivity of electro-thermally poled bioactive silicate glass. J. ActaBiomater. 5(4):1274-1283.
3. Hench LL, Splinter RJ, Allen WC, Greenlee TK (1971) Bonding mechanisms at the interface of ceramic prosthetic materials. J. Biomed. Mater. Res. 5(6):117-141.
4. Cao W, Hench LL (1996) Bioactive materials. J. Ceram. Int. 22(6):493-507.
5. Hench LL (1998) Bioceramics, a clinical success. J. Am. Ceram. Soc. Bull. 77(7):67-74.
6. Day RM, Boccaccini AR, Shurey S, Roether JA, Forbes A, Hench LL, Gabe SM (2004) Assessment of polyglycolic acid mesh and bioactive glass for soft-tissue engineering scaffolds. J. Biomaterials 25(27):5857-5866.
7. Williams DF (1999) The Williams dictionary of biomaterials. Liverpool University Press.

8. El-Meliegy E, van Noort R (2012) Lithium disilicate glass ceramics. In Glasses and Glass Ceramics for Medical Applications (pp. 209-218). Springer, New York, NY.
9. Hench L (2006) The story of Bioglass. J. Mater. Sci. Mater. Med. 17:967-978.
10. Bhakta S, Faira PE, Salata LA, de Oliveira Neto PJ, Miller CA, van Noort R, Hatton PV (2012) Determination of relative in vivo osteoconductivity of modified potassium fluorrichterite glass–ceramics compared with 45S5 bioglass. J. Mater. Sci.: Mater. Med 23(10):2521-2529.
11. Hench LL (1991) Bioceramics: From Concept to Clinic, J Amer. Ceram. Sot, 74, 7.
12. Hench LL (1998) Bioceramics. J Am Ceram Soc 81:1705–28.
13. Hench LL, Polak JM (2002) Third-generation biomaterials. Science 295:1014–7.
14. Ducheyne P, Qiu Q (1999) Bioactive ceramics: the effect of surface reactivity on bone formation and bone cell function. Biomaterials 20:2287–303.
15. Wilson J, Pigott GH, Schoen FJ, Hench LL (1981) Toxicology and biocompatibility of bioglasses. J. Biomed. Mater. Res. 15(6):805-817.
16. Fu H, Rahaman M, Day D, Huang W (2012) Long-term conversion of 45S5 bioactive glass-ceramic microspheres in aqueous phosphate solution. J. Mater. Sci.: Mater. Med. 23:1181- 1191.
17. Xu S, Yang X, Chen X, Shao H, He Y, Zhang L, Yang G, Gou Z (2014) Effect of borosilicate glass on the mechanical and biodegradation properties of 45S5-derived bioactive glass-ceramics. J. Non-Cryst. Solids 405:91-99.
18. Rahaman MN, Day DE, Sonny Bal B, Fu Q, Jung SB, Bonewald LF, Tomsia AP (2011) Bioactive glass in tissue engineering. ActaBiomater. 7:2355-2373.
19. Ascencio JA, Rincon AC, Canizal G (2005) Synthesis and theoretical analysis of samarium nanoparticles: perspectives in nuclear medicine. The Journal of Physical Chemistry B, 109(18), 8806-8812.
20. Ciobanu CS, Iconaru SL, Popa CL, Motelica-Heino M, Predoi D (2015) Evaluation of samarium doped hydroxyapatite, ceramics for medical application:Antimicrobial activity. Journal of Nanomaterials, 2015.
21. Kaur P, Kaur S, Singh GP, Singh DP (2013). Sm^{3+} doped lithium aluminoborate glasses for orange coloured visible laser host material. Solid state communications, 171, 22-25.
22. Rouxel T (2006) Elastic properties of glasses: a multiscale approach. ComptesRendusMécanique, 334(12), 743-753.
23. Singh GP, Kaur S, Kaur P, Singh DP (2012) Modification in structural and optical properties of ZnO, CeO_2 doped Al_2O_3–PbO–B_2O_3 glasses. Physica B: Condensed Matter, 407(8), 1250-1255.
24. Mhareb MHA, Hashim S, Ghoshal SK, Alajerami YSM, Saleh MA, Dawaud RS, Azizan SAB (2014), Impact of Nd^{3+} ions on physical and optical properties of Lithium Magnesium Borate glass. Optical Materials, 37, 391-397.
25. Hidi IJ, Melinte G, Stefan R, Bindea M, Baia L (2013) The study of the structure and bioactivity of the B_2O_3• Na_2O• P_2O_5 system. J. Raman Spectrosc. 44(8):1187-1194.
26. Neuville DR, de Ligny D, Henderson GS (2014) Advances in Raman spectroscopy applied to earth and material sciences. Rev. Mineral. Geochem. 78(1):509-541.
27. Parkinson BG, Holland D, Smith ME, Larson C, Doerr J, Affatigato M, Feller SA, Howes AP, and Scales CR (2008) J. Non-Cryst. / [Solids, 354:1936–42.